The TMEM16A blockers benzbromarone and MONNA cause intracellular Ca^{2+}-release in mouse bronchial smooth muscle cells

Dwivedi, R., Drumm, B. T., Alkawadri, T., Martin, S. L., Sergeant, G. P., Hollywood, M. A., & Thornbury, K. D. (2023). The TMEM16A blockers benzbromarone and MONNA cause intracellular Ca^{2+}-release in mouse bronchial smooth muscle cells. *European Journal of Pharmacology*, *947*, Article 175677. https://doi.org/10.1016/j.ejphar.2023.175677

Published in:
European Journal of Pharmacology

Document Version:
Publisher's PDF, also known as Version of record

European Journal of Pharmacology 947 (2023) 175677

Contents lists available at ScienceDirect

European Journal of Pharmacology

journal homepage: www.elsevier.com/locate/ejphar

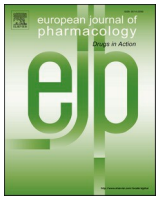

The TMEM16A blockers benzbromarone and MONNA cause intracellular Ca^{2+}-release in mouse bronchial smooth muscle cells

Ritu Dwivedi [a], Bernard T. Drumm [a], Tuleen Alkawadri [a], S. Lorraine Martin [b], Gerard P. Sergeant [a], Mark A. Hollywood [a], Keith D. Thornbury [a,*]

[a] Smooth Muscle Research Centre, Dundalk Institute of Technology, Dublin Road, Dundalk, Co. Louth, Ireland
[b] School of Pharmacy, Queen's University Belfast, Belfast, United Kingdom

A B S T R A C T

We investigated effects of TMEM16A blockers benzbromarone, MONNA, $CaCC_{inh}$A01 and Ani9 on isometric contractions in mouse bronchial rings and on intracellular calcium in isolated bronchial myocytes. Separate concentrations of carbachol (0.1–10 μM) were applied for 10 min periods to bronchial rings, producing concentration-dependent contractions that were well maintained throughout each application period. Benzbromarone (1 μM) markedly reduced the contractions with a more pronounced effect on their sustained component (at 10 min) compared to their initial component (at 2 min). Iberiotoxin (0.3 μM) enhanced the contractions, but they were still blocked by benzbromarone. MONNA (3 μM) and $CaCC_{inh}$A01 (10 μM) had similar effects to benzbromarone, but were less potent. In contrast, Ani9 (10 μM) had no effect on carbachol-induced contractions.

Confocal imaging revealed that benzbromarone (0.3 μM), MONNA (1 μM) and $CaCC_{inh}$A01 (10 μM) increased intracellular calcium in isolated myocytes loaded with Fluo-4AM. In contrast, Ani9 (10 μM) had no effect on intracellular calcium. Benzbromarone and MONNA also increased calcium in calcium-free extracellular solution, but failed to do so when intracellular stores were discharged with caffeine (10 mM). Caffeine was unable to cause further discharge of the store when applied in the presence of benzbromarone. Ryanodine (100 μM) blocked the ability of benzbromarone (0.3 μM) to increase calcium, while tetracaine (100 μM) reversibly reduced the rise in calcium induced by benzbromarone.

We conclude that benzbromarone and MONNA caused intracellular calcium release, probably by opening ryanodine receptors. Their ability to block carbachol contractions was likely due to this off-target effect.

1. Introduction

Ca^{2+}-activated Cl^- channels serve many functions including exocrine secretion, airway epithelial hydration, mucociliary clearance, neuronal and cardiac excitability, sensory signal transduction and smooth muscle excitation (Liu et al., 2021). The molecular identity of these channels was unknown for several decades, but in 2008 three independent research groups provided evidence that it was TMEM16A, a transmembrane protein with previously unknown function (Caputo et al., 2008; Schroeder et al., 2008; Yang et al., 2008). Since then, cryo-electron microscopy and molecular modelling have elucidated the structure-function relationships of the channel pore (Paulino et al., 2017a, 2017b) and research has established the distribution of TMEM16A in a range of tissues that express Ca^{2+}-activated Cl^- currents (Liu et al., 2021). Altered expression or function of TMEM16A is implicated in hypertension, gastrointestinal motility disorders (Liu et al., 2021), asthma (Zhang et al., 2013; Miner et al., 2019), cystic fibrosis (Danahay et al., 2020a, 2020b; Galietta, 2022), neuropathic pain (Deba and Bessac, 2015; Takayama et al., 2015) and cancer (Liu et al., 2021). Consequently, TMEM16A is an attractive drug target for many human diseases, fuelling research to develop new small molecule channel modulators with higher potency and fewer off-target effects than conventional blockers, such as niflumic acid, DIDS (4,49-diisothiocyanatostilbene-2,29-disulfonic acid), NPPB (5-nitro-2-(3--phenylpropylamino) benzoic acid) and 9AC (9-anthracene carboxylic acid). These compounds are generally of low potency and have many off-target effects including modulating intracellular Ca^{2+}-release (see Discussion), activation of large conductance Ca^{2+}-activated K^+ channels (BK_{Ca}) channels (Ottolia and Toro, 1994; Greenwood and Large, 1995), block of K_v4 channels (Wang et al., 1997), L-type Ca^{2+} channel inhibition (Fedigan et al., 2017; Hannigan et al., 2017) and paradoxical activation of Ca^{2+}-activated Cl^- channels (Greenwood and Leblanc, 2007; Bradley et al., 2014). High throughput screening of both 'repurposed' and novel compounds identified a 'second generation' of TMEM16A channel modulators, with higher potencies including $T16A_{inh}$-A01, $CaCC_{inh}$A01, MONNA, niclosamide and Ani9 (De La

* Corresponding author. Dundalk Institute of Technology, Dublin Road, Dundalk, Co. Louth, A91 K584, Ireland.
E-mail address: keith.thornbury@dkit.ie (K.D. Thornbury).

https://doi.org/10.1016/j.ejphar.2023.175677
Received 22 November 2022; Received in revised form 13 March 2023; Accepted 22 March 2023
Available online 24 March 2023

Fuente et al., 2008; Namkung et al., 2011; Huang et al., 2012; Seo et al., 2016; Miner et al., 2019). However, the selectivity of some of these compounds has already been questioned. Boedtkjer et al. (2015) showed that T16A$_{inh}$-A01, CaCC$_{inh}$A01 and MONNA caused vasorelaxation in the absence of extracellular Cl^-, suggesting that their action did not depend on blocking Cl^- channels (Boedtkjer et al., 2015). Also, both T16A$_{inh}$-A01 and CaCC$_{inh}$A01 blocked L-type Ca^{2+} current, though the extent of this seemed to be tissue specific (Cobine et al., 2017; Fedigan et al., 2017; Hannigan et al., 2017). Niclosamide can cause Ca^{2+}-release from intracellular stores and on some published records CaCC$_{inh}$A01 caused an elevation of intracellular Ca^{2+} (Fedigan et al., 2017; Centeio et al., 2020).

At the outset of this study, we began to investigate reported discrepancies in the role of TMEM16A channels in cholinergic contractions of airway smooth muscle. Several studies showed that benzbromarone blocked cholinergic responses in airway smooth muscle (Huang et al., 2012; Zhang et al., 2013; Danielsson et al., 2015). However, despite the fact that TMEM16A is expressed in airway smooth muscle, knockout of *Ano1*, the gene encoding TMEM16A, resulted in little loss of cholinergic responses (Wang et al., 2018). Initially, we speculated that this discrepancy was accounted for by differences in experimental protocols, as our data showed that transient responses to short applications of agonist were blocked less effectively than prolonged contractions in response to longer applications. However, we found that three blockers (benzbromarone, MONNA and CaCC$_{inh}$A01) had a profound off-target effect on intracellular Ca^{2+} regulation. As these drugs are widely used as pharmacological tools to investigate the role of TMEM16A channels in many tissues, any lack of specificity may lead to serious errors in interpretation. Hence, we now report evidence that questions the specificity of these compounds.

2. Materials and methods

2.1. Tissue dissection and cell isolation

All procedures were carried out in accordance with current EU legislation and with the approval of Dundalk Institute of Technology Animal Care and Use Committee (approval 201219). Male and female C57BL/6 mice (10–16 weeks old) were euthanized by intraperitoneal injection of pentobarbitone, and the lungs removed and placed in oxygenated Krebs solution (Solution A). The bronchial tree was exposed by sharp dissection under a microscope to remove surrounding blood vessels and lung tissue. The primary bronchi were removed and cut into small pieces and placed in Hanks Ca^{2+}-free solution (Solution B).

Single airway smooth muscle cells were isolated using a collagenase/proteinase mixture consisting of (per 5 mL of Hanks Ca^{2+}-free solution): 15 mg/ml of collagenase (type II, Sigma Aldrich), 10 mg/ml bovine serum albumin (Sigma Aldrich), 10 mg/ml trypsin inhibitor (Sigma Aldrich) and 1 mg/ml proteinase (Sigma Aldrich). Tissue dissection was performed in Ca^{2+}-free Hanks solution (Solution B). Isolated bronchi were finely chopped into fragments and placed in a Nunclon dish containing Ca^{2+}-free solution, for 5–10 min at room temperature. Tissue fragments were then transferred to a glass test tube for enzymatic cell dispersal, which was performed in two steps. First, tissue fragments were incubated in the primary dispersal medium comprising collagenase, bovine serum albumin and trypsin inhibitor dissolved in Ca^{2+}-free Hanks for 4 min at 37 °C. Next, the secondary dispersal solution containing 1 mg/ml proteinase in Ca^{2+}-free Hanks was added to the primary medium and incubated for a further 3 min at 37 °C. During the dispersal, tissue fragments were mechanically stirred using a magnetic stir bar and gently triturated using a glass pipette to aid the release of single airway smooth muscle cells. After 7 min of treatment with the enzyme mixture, the solution was centrifuged for 30 s. The supernatant was discarded and Ca^{2+}-free Hanks was used to wash the enzyme treated tissue fragments. The glass tube containing tissue fragments and 4 ml of Ca^{2+}-free Hanks was placed in a water bath (37 °C) and the solution was gently triturated for 10 min to isolate airway smooth muscle cells. Isolated cells were stored at 4 °C and utilised within the same day.

2.2. Isometric tension recordings

Rings, 1–2 mm in length, from mouse primary bronchi were mounted in water-jacketed organ baths, perfused with warmed Krebs solution (Solution A) and, adjusted to 5 mN tension (based on previous pilot experiments) and allowed to equilibrate for 40 min. Isometric contractions were measured using a Myobath system and data were acquired using DataTrax 2 software (WPI, Hitchin, Hertfordshire, UK). Drugs were made up to a stock concentration in an appropriate solvent, as per the manufacturer specifications. Stock solutions were then delivered to the organ bath, where they were diluted in Krebs solution to their final concentration. All isometric tension experiments presented in this study were carried out in the presence of indomethacin (COX 1/2 inhibitor, 10 μM) to prevent modulation caused by release of endogenous prostaglandins from epithelial cells (Butler et al., 1987).

2.3. Ca^{2+} imaging

Cells were plated and incubated in 0.4 μM fluo-4AM (Molecular Probes) for 6–8 min at room temperature in Hank's Ca^{2+}-free solution to which 100 μM Ca^{2+} was added. During experiments, dishes containing cells were continuously perfused with Hanks solution (Solution C) at 35 ± 2 °C. Additionally, the cell under study was continuously superfused with Hanks solution by means of a custom built close delivery system with a pipette tip diameter of 200 μm placed approximately 300 μm from the cell. The Hanks solution in the close delivery system could be switched to a drug-containing solution with a dead-space time of less than 5 s.

Cells were imaged using an iXon 887 EMCCD camera (Andor Technology, Belfast, UK; 512 x 512 pixels, pixel size 16 x16 μm) coupled to a Nipkow spinning disk confocal head (CSU22, Yokogawa, Japan). A solid state 50 mW 488 nM laser (ANDOR Technology) was used to excite Fluo-4 and the emitted light was detected at wavelengths >510 nm. Experiments were performed using a x60 objective (Olympus) resulting in images of pixel size 0.266 x 0.266 μm. Images were acquired at 15 frames per second (FPS) and analysed using ImageJ software (version 1.48, National Institutes of Health, Bethesda, MD) as described previously (Drumm et al., 2019a). Background fluorescence from the camera, obtained using a null frame, was subtracted from each frame to obtain 'F'. F_0 was determined as the minimum fluorescence measured between Ca^{2+} responses. To obtain *post-hoc* pseudo line-scan images for display in figures, a one pixel thick line was drawn centrally through the entire length of the cell and the "Reslice" command in Image J was invoked. Plots of the fluorescence (F) were normalized by dividing by F_0. Plots of F/F_0 against time were obtained from the *post-hoc* line-scan by drawing a rectangle around the entire area of the line-scan image and plotting the intensity profile in Image J. The amplitudes of Ca^{2+} events were obtained from the intensity profile plot as the change in F/F_0 units, $\Delta F/F_0$, measured as the difference between the peak and baseline.

2.4. Solutions

The following solutions were used. Concentrations in mM are given in parentheses.

A. Krebs Solution for isometric tension recording (mM): NaCl (120), KCl (5.9), $NaHCO_3$ (25), $NaH_2PO_4.2H_2O$ (1.2), glucose (5.5), $MgCl_2$ (1.2), $CaCl_2$ (2.5), pH was adjusted to 7.4 by bubbling the solution with 95% O_2 – 5% CO_2 continuously.
B. Ca^{2+} free Hanks solution for cell dispersal (mM): NaCl (125), KCl (5.4), glucose (10), sucrose (2.9), $NaHCO_3$ (4.2), KH_2PO_4 (0.4), NaH_2PO_4 (0.3), HEPES (10). pH was adjusted to 7.4 using NaOH.

C. Hanks, bath solution for Ca^{2+} imaging (mM): NaCl (125), KCl (5.36), glucose (10), sucrose (2.9), $NaHCO_3$ (4.17), KH_2PO_4 (0.44), NaH_2PO_4 (0.33), $MgCl_2.6H_2O$ (0.5), $CaCl_2.2H_2O$ (1.8), $MgSO_4.7H_2O$ (0.4), HEPES (10), pH adjusted to 7.4 with NaOH.

D. Ca^{2+} free Hanks superfusate solution (mM): NaCl (125), KCl (5.36), glucose (10), sucrose (2.9), $NaHCO_3$ (4.17), KH_2PO_4 (0.44), Na_2HPO_4 (0.33), $MgCl_2.6H_2O$ (2.3), EGTA (5.0), $MgSO_4.7H_2O$ (0.4), HEPES-free acid (10), pH to 7.4 with NaOH.

2.5. Drugs

Carbachol, ryanodine and tetracaine (Sigma-Aldrich), benzbromarone, $CaCC_{inh}A01$, MONNA and Ani9 and cyclopiazonic acid (CPA) (Tocris), iberiotoxin (Smartox), nifedipine (Ascent Scientific), indomethacin (Abcam). Carbachol, tetracaine and iberiotoxin were solubilised in water. Dimethyl sulfoxide (DMSO) was used to solubilise benzbromarone, $CaCC_{inh}A01$, MONNA, Ani9, ryanodine and CPA. The maximal concentration of DMSO in these cases (except ryanodine) was 0.1%. For ryanodine, the maximal concentration of DMSO was 1%. Ethanol was used to solubilise nifedipine and indomethacin. The maximal concentration of ethanol was 0.1%. The maximal DMSO and ethanol, in concentrations used to solubilise drugs, had no effect on tension or intracellular Ca^{2+}.

2.6. Statistical analysis

With the exception of the data in Fig. 4B & C, experimental data sets were performed on a minimum of six animals (N). In Fig. 4B and C, 6 cells from 3 animals were used. Data were analysed using Graphpad Prism software. Summarised data are presented as mean ± standard error of the mean (SEM). Tension graphs were compared using 2-way ANOVA, with Bonferroni's post hoc test. Ca^{2+}-imaging data comprising 2 sets were compared using Wilcoxon's matched pairs signed rank test, while data comprising 3 sets were compared using Friedman's test followed by Dunn's test for multiple comparisons. Differences were considered as statistically significant if $p < 0.05$.

3. Results

3.1. Effect of TMEM16A blockers on isometric tension

The effect of benzbromarone (1 μM), a TMEM16A blocker, was examined on contractures of mouse bronchi induced by carbachol (CCh, 0.1–10 μM), where each CCh concentration was applied separately for

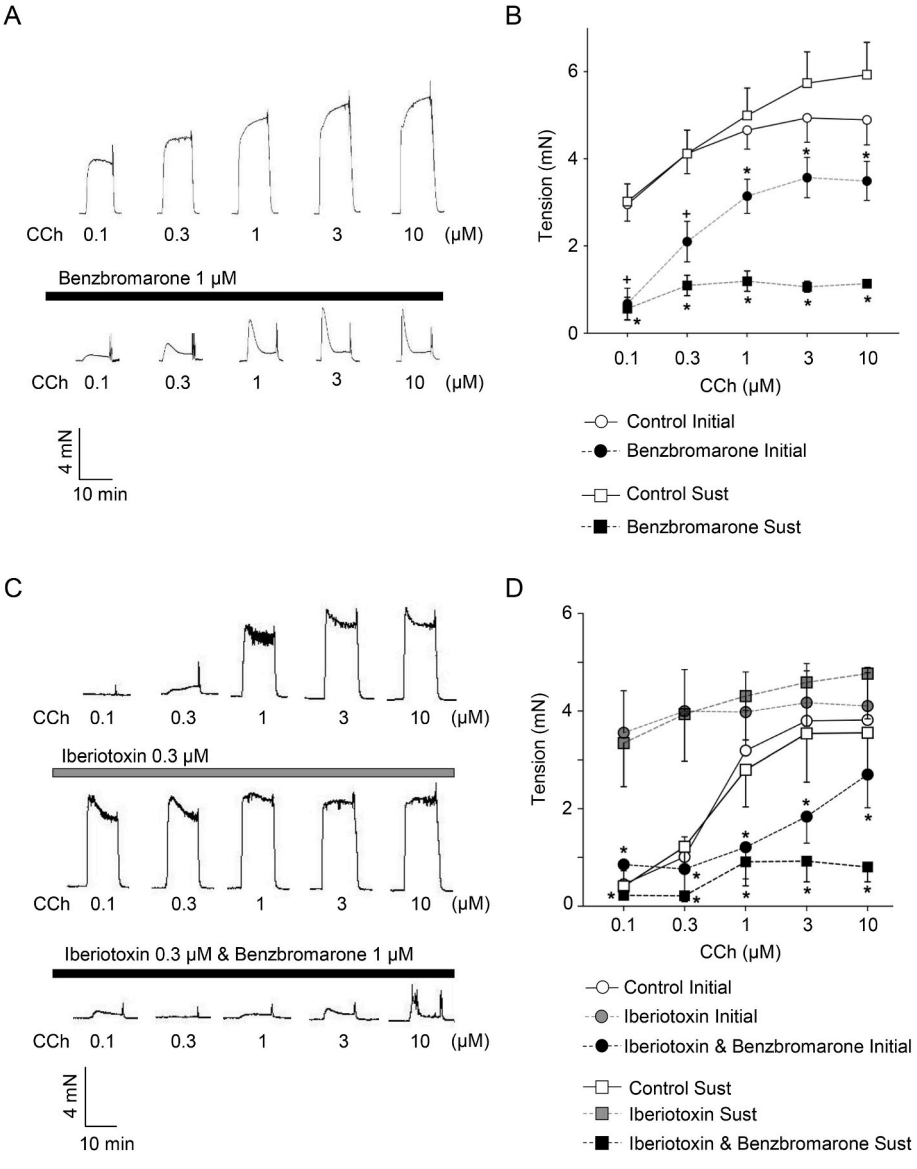

Fig. 1. Effect of benzbromarone on carbachol-induced contractions. **A**, isometric tension recording taken from a bronchial ring response to separate 10 min applications of carbachol (CCh; 0.1–10 μM) in control conditions (upper panel) and in the presence of benzbromarone (1 μM; lower panel). **B**, summary of the effect of benzbromarone on the carbachol concentration-effect curve for initial contractions (measured after 2 min exposure to carbachol) and the sustained contraction (Sust; measured at the end of 10 min exposure to carbachol), n = 6 bronchial rings from 6 animals. **C**, separate applications of increasing concentrations of carbachol (0.1–10 μM) in control (top panel), iberiotoxin (0.3 μM; middle panel) and benzbromarone and iberiotoxin (1 μM; bottom panel). **D**, summary of the effect of benzbromarone on the carbachol in the presence of iberiotoxin, n = 6 bronchial rings from 6 animals. Format as in B. *P < 0.0001, $^{+}$P < 0.02.

10 min and then washed out. Fig. 1A shows that each concentration of CCh produced a well-sustained contraction. Sometimes the initial phase of the contraction was of smaller amplitude than the contraction measured at the end of the 10 min, as in Fig. 1A (and Fig. 2C), although at times the initial phase was greater (e.g. Figs. 1C and 2A). After washout of 10 μM CCh, benzbromarone was then applied for 30 min before repeating the CCh applications. Benzbromarone effectively reduced the responses to all concentrations of CCh and, notably, it had more effect on the sustained component of contraction than the initial phase, except at 0.1 μM of CCh, where it was equally effective on both components. Data from six experiments are presented in Fig. 1B, where benzbromarone significantly reduced the responses to CCh at all concentrations, again with greater effect on the sustained components of the contractions.

As several blockers of Ca^{2+}-activated Cl^- channels, including benzbromarone, have been shown to directly activate BK_{Ca} channels (Ottolia and Toro, 1994; Gao et al., 2023), a series of experiments were performed to examine benzbromarone's effects in the presence of iberiotoxin (0.3 μM), a potent BK_{Ca} channel-inhibitor. Fig. 1C shows the effect of CCh applications, first in the absence of iberiotoxin (top panel), then in its presence (middle panel) and then in the presence of iberiotoxin and benzbromarone (bottom panel). Iberiotoxin greatly potentiated the CCh contractions, especially at lower concentrations of CCh (Fig. 1C–D). Benzbromarone effectively blocked all of these enhanced contractions (Fig. 1C–D), indicating that its effect was not mediated by opening BK_{Ca} channels.

Two other TMEM16A inhibitors, MONNA (3 μM) and $CaCC_{inh}A01$ (10 μM) had broadly similar blocking effects to benzbromarone, although they were less potent (Fig. 2A–B and Figs. S1A and S2B). In contrast, Ani9, even in high concentration (10 μM) relative to its IC_{50} for TMEM16A (0.1 μM (Seo et al., 2016)), had no effect on CCh contractions at any concentration of the agonist (Fig. 2C–D). Wang et al. (2018) showed that in TMEM16A knockout mice, cholinergic responses were well-preserved in airway smooth muscle but responses to other agonists, including U-44619, a thromboxane agonist, were severely impaired (Wang et al., 2018). Therefore, we checked if Ani9 was able to antagonise contractions in response to this agonist. U-44619 (0.1 μM) typically caused phasic contractions which were effectively antagonised by Ani9 (3 μM; Fig. S2). Hence, the lack of effect of Ani9 against CCh contractions could not be attributed to lack of tissue potency of this compound.

The lack of contractile impairment from cholinergic agonists in TMEM16A knockout mice (Wang et al., 2018), combined with the fact that in the present study, Ani9 had no effect on CCh-induced contractions in wild type mice, led us to suspect that the inhibition produced by the other three blockers was due to off-target effects. This was reinforced by the finding that they were equally effective at blocking cholinergic contractions after exposing the tissue to nifedipine (Fig. S3). If, as has been assumed, TMEM16A channels cause bronchoconstriction by depolarising the smooth muscle cell membrane and activating L-type Ca^{2+} channels, then TMEM16A blockers should have no further action after blocking L-type channels.

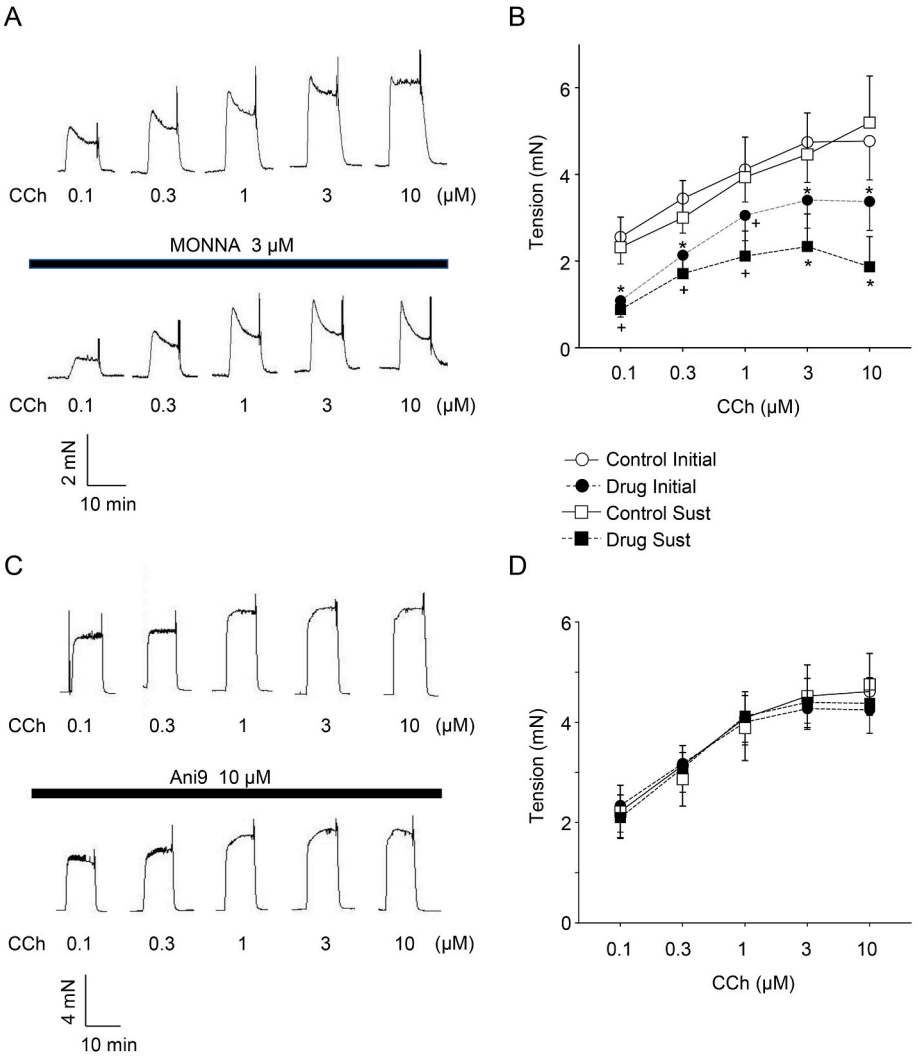

Fig. 2. Effect of MONNA and Ani9 on carbachol-induced contractions. **A**, isometric tension recording of contractions in response to separate 10 min applications of carbachol (CCh; 0.1–10 μM) in control conditions (upper panel) and in the presence of MONNA (3 μM; lower panel). **B**, summary of the effect of MONNA on the carbachol concentration-effect curve. Initial contractions and sustained (Sust) contractions defined as in Fig. 1B, n = 6 bronchial rings from 6 animals. **C**, contractions in response to carbachol (0.1–10 μM) in control conditions (upper panel) and in the presence of Ani9 (10 μM; lower panel). **D**, summary of the effect of Ani9 on the carbachol concentration-effect curve, n = 6 bronchial rings from 6 animals. *P < 0.0001, $^{+}$P < 0.01.

3.2. Effect of TMEM16A blockers on cytosolic Ca^{2+}

Since several TMEM16A blockers have been observed to modulate intracellular Ca^{2+} (see Discussion), we decided to examine the effects of the TMEM16A compounds on cytosolic [Ca^{2+}] in isolated cells. Fig. 3A shows a pseudolinescan image obtained an isolated bronchial smooth muscle cell recording and below this is a profile plot of the changes cytosolic Ca^{2+} on the same time scale, normalized to resting level as F/F_0. Benzbromarone (0.3 μM) was applied three times for 30 s, and each time it caused a reversible increase in F/F_0. In six similar experiments, benzbromarone caused reproducible elevations in Ca^{2+} ($\Delta F/F_0$) over the 3 applications (Fig. 3B). Preliminary experiments also showed that benzbromarone at 1 μM resulted in an elevated cytosolic Ca^{2+}, but this was slow to wash out over the time course of the experiment. Next, we determined if the effect of benzbromarone was due to increased Ca^{2+} entry across the plasma membrane, or if it could be explained by release from intracellular Ca^{2+} stores. Fig. 3C shows an example, where benzbromarone (0.3 μM) was applied first in normal extracellular Ca^{2+}, then after 30 s exposure to Ca^{2+}-free conditions and then again in normal Ca^{2+}. Application of the Ca^{2+}-free solution decreased basal Ca^{2+}. When benzbromarone was applied under this condition it still produced an increase in F/F_0. Data from six similar experiments are presented in

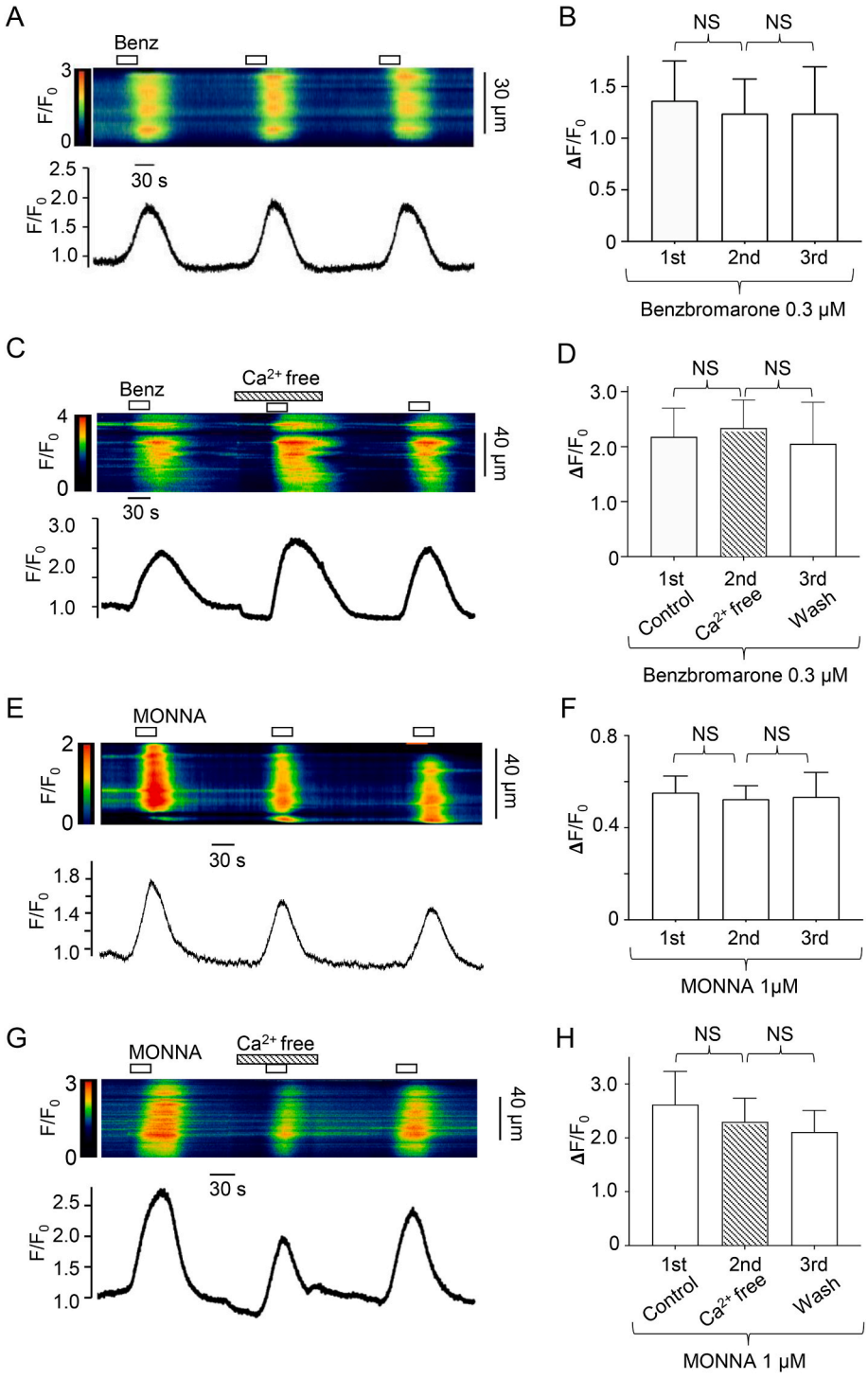

Fig. 3. Effect of benzbromarone (Benz) and MONNA on intracellular Ca^{2+}. **A**, pseudolinescan (upper panel) derived from a movie showing the effect of three applications of benzbromarone (0.3 μM) to a single bronchial myocyte. The amplitudes of Ca^{2+} events are shown in the intensity profile plot (lower panel), derived from the linescan in F/F_0 units. **B**, summary of the effect of 3 successive applications of benzbromarone, n = 6 cells from 6 animals. **C**, effect of Ca^{2+}-free extracellular solution on the effect of benzbromarone. The 1st and 3rd applications of benzbromarone were in normal extracellular Ca^{2+}, while the 2nd application was in Ca^{2+}-free conditions. **D**, summary of the effect of Ca^{2+}-free extracellular solution on the effect of benzbromarone, n = 6 cells from 6 animals. The 1st (Control) and 3rd (Wash) applications were in normal Ca^{2+}, while the 2nd was in Ca^{2+}-free. **E**, effect of 3 applications of MONNA (1 μM) in a single myocyte, format as in A. **F**, summary of the effect of 3 application of MONNA to single cells, n = 6 cells from 6 animals, format as in B. **G**, effect of Ca^{2+}-free extracellular solution on the effect of MONNA. Format as in C. **H**, summary of the effect of Ca^{2+}-free extracellular solution on the effect of MONNA, n = 7 cells from 7 animals. Format as in D. NS = no statistically significant difference.

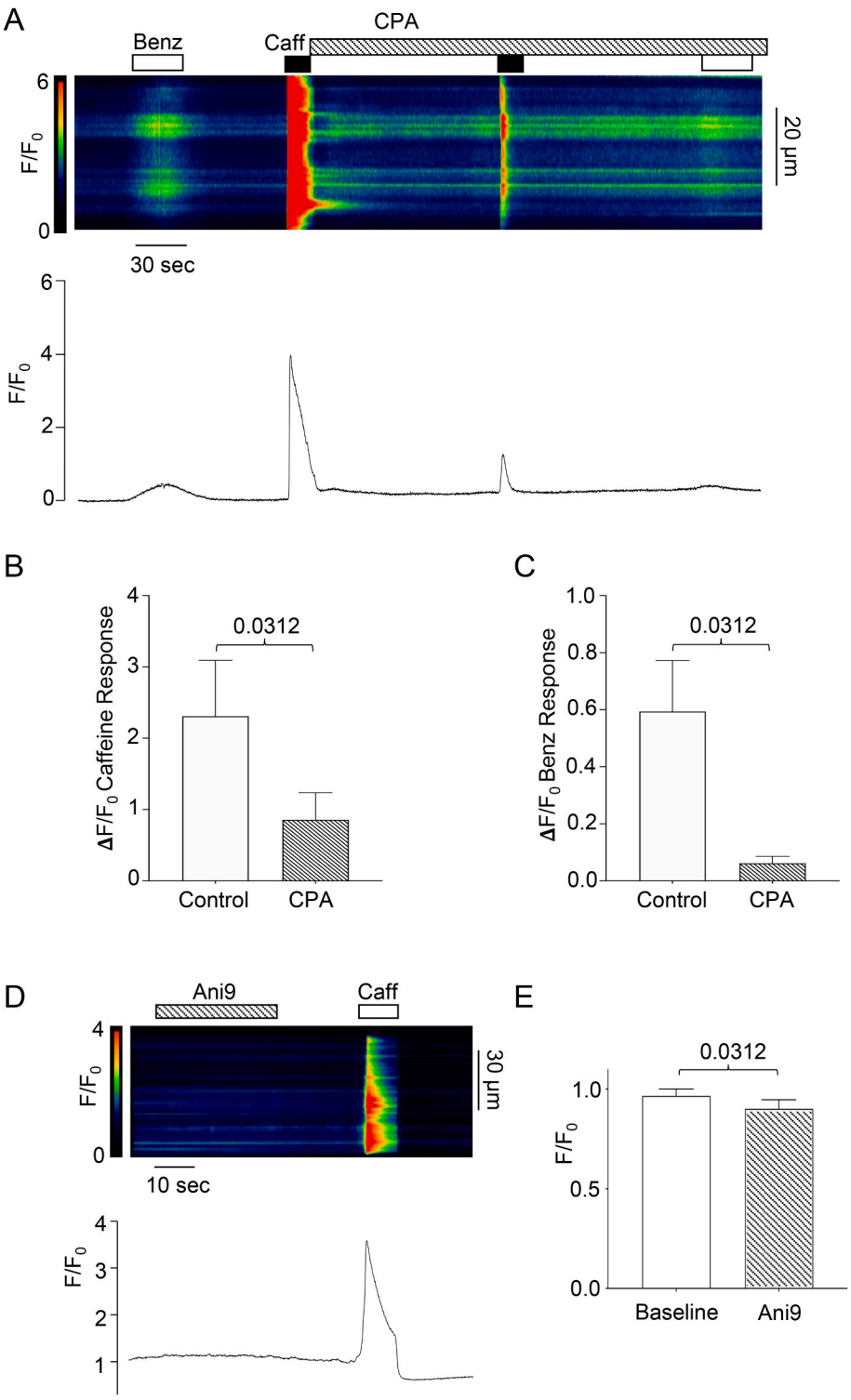

Fig. 4. A-C, Effect of CPA on Ca^{2+} elevations elicited by benzbromarone (Benz) and caffeine (Caff). A, pseudolinescan (upper panel) derived from a movie showing the effect of benzbromarone (0.3 μM) and caffeine (10 mM) on a single bronchial myocyte. After wash of caffeine, CPA (10 μM) was applied and the caffeine and benzbromarone applications were repeated. The amplitudes of Ca^{2+} events are shown in the intensity profile plot (lower panel), were derived from the linescan in F/F_0 units. B & C, summaries of the effect of CPA on the caffeine and benzbromarone responses in n = 6 cells from 3 animals. D & E, effect of Ani9 (10 μM) on intracellular Ca^{2+}. D, Psuedolinescan (upper panel) derived from a movie showing the effect of Ani9 (10 μM) to a single bronchial myocyte for 30 s. For comparison, caffeine (10 mM) was added after wash out of Ani 9. The amplitudes of Ca^{2+} events are shown in the intensity profile plot (lower panel), were derived from the linescan in F/F_0 units. E, summary of the effect of Ani9, n = 6 cells from 6 animals. The decrease in Ca^{2+} in the presence of Ani9 was trivial (<7%), but statistically significant as shown (Wilcoxon matched-pairs signed rank test).

Fig. 3D, where there was no difference if benzbromarone applied in normal extracellular Ca^{2+} (Control), Ca^{2+}-free solution or following restoration of extracellular Ca^{2+} (Wash). These results strongly suggest that the effect was due to release of Ca^{2+} from intracellular stores. MONNA (1 μM) also elicited similar reproducible increases in cytosolic Ca^{2+} to benzbromarone (Fig. 3E–F), and these also were evident in Ca^{2+}-free extracellular bath solution. Although the $\Delta F/F_0$ appeared slightly reduced in the example shown, the effect of MONNA was still substantial (Fig. 3G). Overall, no significant differences were found in six experiments (Fig. 3H).

To further investigate the effect of the store on the response to benzbromarone, the effect of CPA, a SERCA pump blocker was tested. First, the effects of benzbromarone (0.3 μM) and caffeine (10 mM), which is known to open ryanodine receptors and release Ca^{2+}, were compared (Fig. 4A). Both caused an elevation in Ca^{2+} though, notably, the effect of caffeine was much greater. On washout of caffeine, CPA (10 μM) was applied to prevent Ca^{2+} refilling of the sarcoplasmic reticulum, and then the caffeine and benzbromarone applications were repeated. Both responses were greatly attenuated in the presence of CPA. The effects of CPA on caffeine and benzbromarone responses in 6 cells are

summarised in Fig. 4B & C. We also demonstrated that $CaCC_{inh}A01$ (10 μM) could increase cytosolic Ca^{2+}, but we did not study this effect further (Fig. S4). In contrast, Ani9 (10 μM) did not increase intracellular Ca^{2+} (Fig. 4D & E).

The effects of benzbromarone and MONNA on cytosolic Ca^{2+} were studied further following depletion of the sarcoplasmic reticulum with caffeine. Fig. 5A shows a record where caffeine (10 mM) caused a typical sharp increase in cytosolic Ca^{2+}, followed by a slowly declining plateau that persisted during caffeine exposure. On wash out, the Ca^{2+} returned to the basal level. The caffeine application was repeated approximately 3 min later (indicated by the gap in the record) and this time benzbromarone was applied during the plateau phase, when the store would be expected to be Ca^{2+}-depleted. In this condition, benzbromarone (0.3 μM) elicited little or no further increase in Ca^{2+}, consistent with the conclusion that its effect depended on Ca^{2+} release from the store. A summary eight similar experiments confirmed this result, where there was no significant difference in the $\Delta F/F_0$ during the plateau phase of the caffeine response in the presence or absence of benzbromarone (Fig. 5B). In these experiments the peak Ca^{2+} response was 4.3 ± 1.7 $\Delta F/F_0$ units (not shown on graph). Similar experiments were performed for MONNA (1 μM), where it also failed to elicit a further response in the presence of caffeine (Fig. 5C–D). The peak Ca^{2+} response to caffeine in these experiments was 4.0 ± 1.7 $\Delta F/F_0$ (n = 6 from 6 animals, data not shown).

Taken together, the above experiments suggest that the actions of benzbromarone and MONNA were due to Ca^{2+}-release from the sarcoplasmic reticulum. If true, we hypothesised that caffeine may not be able to evoke much further release if applied in the presence of benzbromarone. In the experimental record shown in Fig. 6A, benzbromarone was applied at a higher concentration of 1 μM to produce a sustained response and caffeine (10 mM) was then applied for 20s. Under these conditions, caffeine decreased the elevated level caused by benzbromarone, rather than evoking the usual increase in F/F_0. In six similar experiments, $\Delta F/F_0$ in benzbromarone plus caffeine was significantly less than in benzbromarone alone (Fig. 6B).

To test the idea that benzbromarone might raise cytosolic Ca^{2+} by opening ryanodine receptors on the sarcoplasmic reticulum, we examined the effect of two blockers of these channels. Firstly, we tested the effect of ryanodine, the classical, but irreversible blocker (MacMillan et al., 2005). Initially, benzbromarone (0.3 μM) was applied for 30 s, where it increased cytosolic Ca^{2+} (Fig. 7A). As the onset of block with ryanodine is known to be slow compared to tetracaine (MacMillan et al., 2005), its effects on benzbromarone were tested by preincubating the cells with ryanodine. Hence, after washout of benzbromarone, ryanodine (100 μM) was applied for 90 s and then benzbromarone was applied again in the presence of ryanodine, where it caused only a very small Ca^{2+} transient (Fig. 7A). Summary data in 6 cells confirmed that ryanodine almost completely blocked the effect of benzbromarone (Fig. 7B).

Next, we examined the effect of tetracaine, a reversible blocker of ryanodine receptors with rapid kinetics (Sergeant et al., 2009). As ryanodine receptor blockade with tetracaine is known to be transient and fades with continuous application (Sergeant et al., 2009; Viero et al., 2012), tetracaine was applied after benzbromarone had already caused an elevation in Ca^{2+}, rather than preincubating with tetracaine and then observing the effect of benzbromarone. Tetracaine (100 μM) was applied

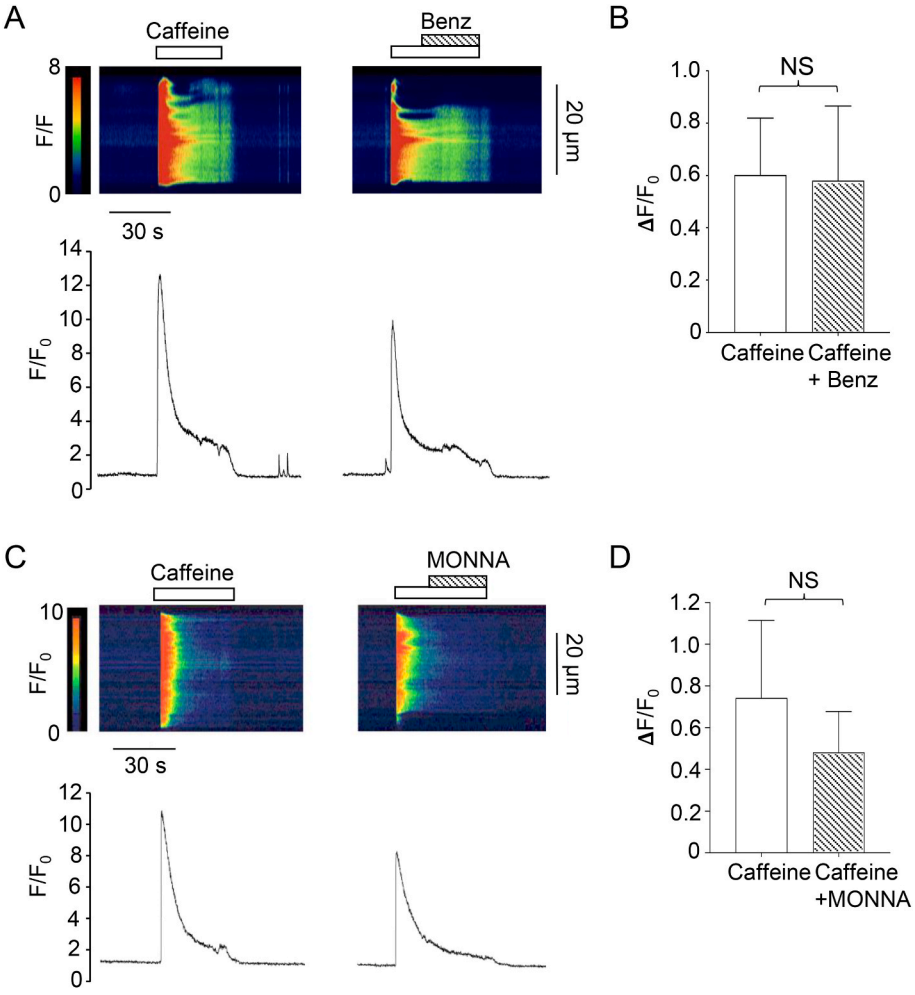

Fig. 5. Effect of benzbromarone (Benz) in the presence of caffeine. **A**, pseudolinescan and intensity profile plot from a single cell showing 30 s applications of caffeine (10 mg) alone and then with benzbromarone. Typically, caffeine caused a peak in Ca^{2+} followed by a plateau phase. Caffeine was washed out and the applied a 2nd time after 60 s. Benzbromarone (0.3 μM) was applied during the plateau phase of the 2nd caffeine response. **B**, summary of the effect of benzbromarone applied during the plateau phase of the caffeine response, n = 8 cells from 8 animals. **C**, pseudolinescan and intensity profile plot from a single cell showing 30 s applications of caffeine alone and then with MONNA (1 μM). Format as in A. **D**, summary of the effect of MONNA applied during the plateau phase of the caffeine response, n = 6 cells from 6 animals. Format as in B. NS = no statistical differences.

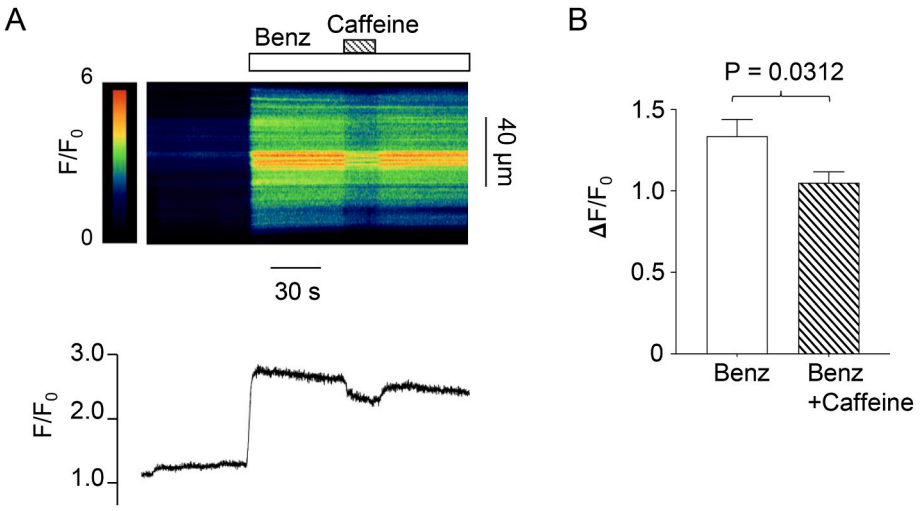

Fig. 6. Effect of caffeine in the presence of benzbromarone (Benz). **A**, pseudolinescan and intensity profile plot showing benzbromarone (1 μM) applied to a single cell for ~8 min, during which caffeine (10 mg) was applied for a period of 30 s. Caffeine failed to increase Ca^{2+} in the presence of benzbromarone and indeed, decreased Ca^{2+} slightly. **B**, summary showing that caffeine caused a small but significant decrease in Ca^{2+} from the elevated level in benzbromarone. n = 6 cells from 6 animals.

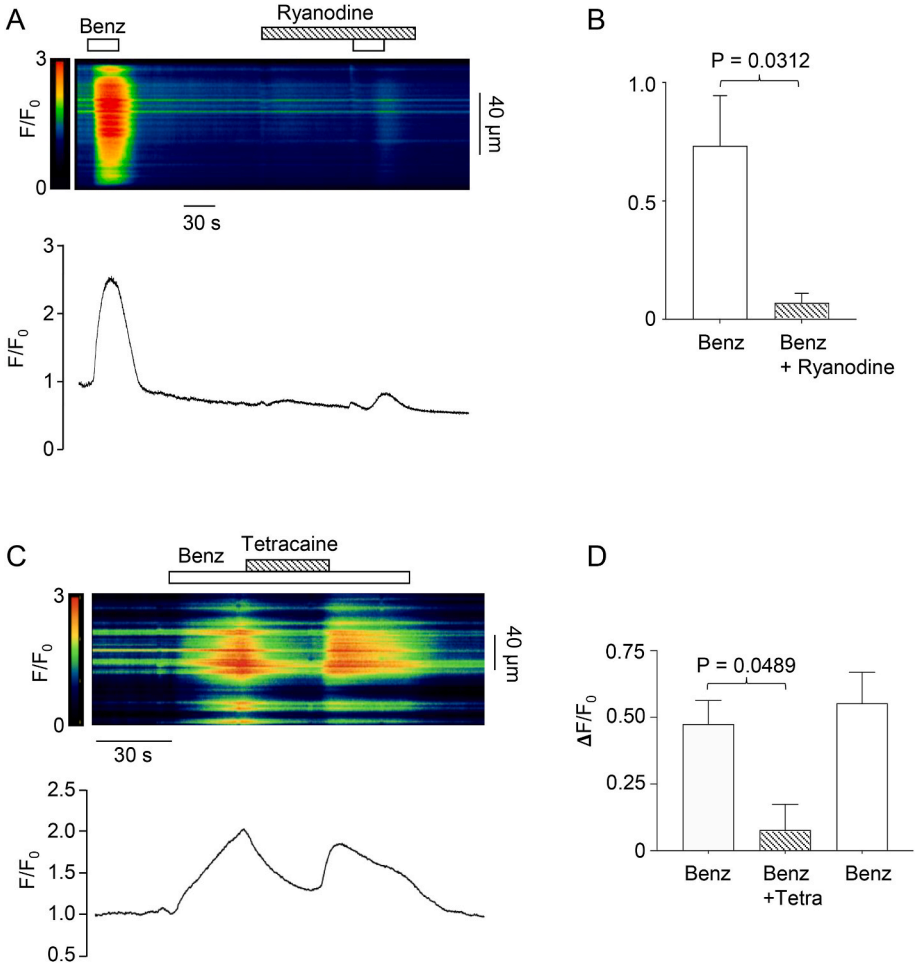

Fig. 7. The effect of blocking ryanodine receptors on the response to benzbromarone (Benz). **A**, pseudolinescan and intensity profile plot showing benzbromarone (0.3 μM) applied for 30 s to a single cell and ten washed out. Ryanodine (100 μM) was applied after 2 min and 30 s later benzbromarone was applied for a 2nd time. **B**, summary of the effect of ryanodine on the response to benzbromarone, n = 6 cells from 6 animals. **C**, pseudolinescan and intensity profile plot showing a 90s addition of benzbromarone (0.3 μM). During the middle 30 s of the benzbromarone addition, tetracaine (100 μM) was added and then removed. Tetracaine reversibly reduced the elevation in Ca^{2+} caused by benzbromarone. D, summary of the effect of tetracaine on the benzbromarone response, n = 8 cells from 8 animals.

for 30 s in the middle of a 90 s application of benzbromarone (0.3 μM), where it rapidly and reversible reduced F/F_o from the elevated level induced by benzbromarone (Fig. 7C). Summary data from eight similar experiments confirmed that tetracaine reversibly reduced the effect of benzbromarone (Fig. 7D).

4. Discussion

Patch clamp studies established that native airway smooth muscle cells possessed Ca^{2+}-activated Cl^- channels activated by acetylcholine (Janssen and Sims, 1992), and later TMEM16A was shown to be expressed in airway smooth muscle cells (Huang et al., 2009, 2012; Gallos et al., 2013; Zhang et al., 2013). Knockout of TMEM16A in mice resulted in attenuation of responses of bronchial smooth muscle to U-44619 and 5-hydroxytryptamine, but contractions evoked by the cholinergic agonist methacholine were well preserved (Wang, 2018). The present study was prompted by the fact that the survival of robust cholinergic contractions in TMEM16A knockout mice appeared to be at odds with the ability of benzbromarone and niclosamide to block cholinergic contractions (Huang et al., 2012; Danielsson et al., 2015; Miner et al., 2019). We hypothesised that TMEM16A channels were involved in sustaining cholinergic contractions, but were less important for transient contractions, therefore the discrepancies in the published studies might be attributable to differences in experimental protocols. Initially, this appeared to be confirmed, as benzbromarone, MONNA and $CaCC_{inh}$A01, blocked the sustained component of carbachol-induced contractions more than the initial component. However, several observations made us doubt the specificity of the TMEM16A blockers. First, we found that these compounds were still effective in tissues that had been treated with nifedipine (Fig. S3). Second, Ani9, had no effect on carbachol-induced contractions (Fig. 2C), even though it effectively reduced phasic contractions induced by U-44619 (Fig. S2). Others have found Ani9 (Seo et al., 2016) to be a potent TMEM16A blocker in whole tissue preparations of gastrointestinal smooth muscle (Drumm et al., 2019b, 2019c, 2020a, 2020b, 2022; Koh et al., 2022), including specifically reducing cholinergic induced contractions of proximal colon muscles (Drumm et al., 2020a). Its lack of effect in the present study supports the idea that TMEM16A channels contribute little to cholinergic contractions in airway smooth muscle, at least under normal (non-inflammatory) conditions. Interestingly, another study found that Ani9 failed to dilate human bronchi *in vitro* and came to the same conclusion (Danahay et al., 2020a).

We show that benzbromarone, MONNA and $CaCC_{inh}$A01, but not Ani9, elevated cytosolic Ca^{2+} in mice bronchial myocytes. This effect was investigated further for benzbromarone and MONNA, where we found that it still occurred when extracellular Ca^{2+} was removed, indicating that it was due to release from intracellular stores. The role of the sarcoplasmic reticulum store was investigated by examining the effects of caffeine, which opens ryanodine receptors, as well as tetracaine and a high concentration of ryanodine, which act as reversible and irreversible blockers of ryanodine receptors, respectively (Nagasaki and Fleischer, 1988; Gyorke et al., 1997). Benzbromarone and MONNA did not elevate Ca^{2+} further when the ryanodine receptors were already opened by caffeine. Conversely, caffeine was unable to elevate Ca^{2+} in the presence of benzbromarone. These effects are consistent with the idea that benzbromarone and caffeine had a similar action in opening ryanodine receptors, and this is supported by the fact that tetracaine and ryanodine were able to attenuate the elevation of Ca^{2+} caused by benzbromarone. Elevations in Ca^{2+} due to IP_3 activation or SERCA pump blockade would be less likely to be so effectively attenuated by tetracaine and ryanodine. Interestingly, the effect of caffeine was reversed in the presence of benzbromarone, where it caused a small reduction in Ca^{2+}. We speculate that this was due to caffeine's well-known action as a phosphodiesterase inhibitor, boosting intracellular cAMP levels over the same concentration range that it activates ryanodine receptors (Faudone et al., 2021). Phospholamban is known to regulate the SERCA pump in airways smooth muscle (Sathish et al., 2008), thus cAMP-dependent phosphorylation of phospholamban, would be expected to result in disinhibition of the sarcoplasmic/endoplasmic reticulum Ca^{2+}-ATPase (SERCA) pump, causing Ca^{2+} sequestration (Simmerman and Jones, 1998). Normally, this Ca^{2+}-sequestration would be masked by the more powerful Ca^{2+}-releasing effect of caffeine.

Although we have observed direct contractile effects of high concentrations of benzbromarone (e.g. 10 mM, data not shown), it is puzzling that we did not see contractile effects of these drugs at the concentrations required to block carbachol responses. Also, in single cell Ca^{2+} imaging experiments most cells did not contract upon application of these drugs but did with caffeine. One possible reason for this might be that the degree of Ca^{2+} release caused by the TMEM16A blockers was usually less than that released by caffeine (e.g. compare responses in Fig. 4A). It may be that a slow gradual release of Ca^{2+} in the tension experiments was insufficient to cause contraction, but nevertheless depleted the Ca^{2+} store enough to affect responses to carbachol. Alternatively, it is possible that these drugs inhibited contractions by additional off-target effects such as interfering with contractile proteins or their Ca^{2+}-sensitivity. However, this seems less likely, as it would not explain the tendency of the drugs to block the sustained component of the carbachol-induced contractions, compared to the initial component.

Several other studies have indicated that some classical Ca^{2+}-activated Cl^- blockers and new generation TMEM16A blockers can cause intracellular Ca^{2+}-release. Cruickshank et al. (2003) showed that niflumic acid, DIDs, NPPB and 9AC elevated cytosolic Ca^{2+} in rat pulmonary artery smooth muscle cells and cited examples of similar effects in visceral smooth muscle cells, epithelial cells, a salivary epithelial cell line (ST885 cells), and neurons (Cruickshank et al., 2003). More detailed analysis of the effect of niflumic acid showed that it caused Ca^{2+}-release from intracellular stores via a ryanodine receptor-dependent mechanism. Of the new generation compounds, we previously noted that $CaCC_{inh}$A01 increased cytosolic Ca^{2+} in rabbit urethral interstitial cells of Cajal (Fedigan et al., 2017), while niclosamide was reported to cause intracellular Ca^{2+} release in HT_{29} human colonic carcinoma epithelial cells (Centeio et al., 2020). Benzbromarone has, so far, not been reported to release intracellular Ca^{2+}, but Danielsson et al. (2015) found that high concentrations (50 &100 μM) blocked the ability of bradykinin and histamine to elevate intracellular Ca^{2+} in human airway smooth muscle cells bathed in Ca^{2+}-free extracellular solution (Danielsson et al., 2015). Their study also reported that agonist-induced changes in mag-fluo-4 fluorescence were attenuated by both benzbromarone and MONNA, suggestive of interference with sarcoplasmic reticulum Ca^{2+}-release by these drugs. At the time of writing, Genovese et al. presented evidence that $CaCC_{inh}$A01 and MONNA interfered with Ca^{2+} mobilisation by several agonists and release of caged IP_3 in several cell lines (Genovese et al., 2023). In contrast to the present study, these investigators did not observe elevations in Ca^{2+} induced by $CaCC_{inh}$A01 or MONNA, though they did so with niclosamide. They proposed that $CaCC_{inh}$A01 blocked IP_3-mediated Ca^{2+}-release, although it also reduced Ca^{2+} elevations with ionomycin, which released Ca^{2+} from the store without activating plasmalemmal receptors, suggesting that it had multiple effects on Ca^{2+} mobilisation. As in the present study, Genovese et al. reported that Ani9 did not interfere with Ca^{2+} mobilisation or block agonist effects.

The fact that so many diverse Ca^{2+}-activated Cl^- channel blockers cause intracellular Ca^{2+} release suggests that they may share a common molecular target, besides plasmalemmal TMEM16A. Ca^{2+} movements across the sarcoplasmic reticulum cannot be sustained unless electrical charge neutrality is maintained by movement of a counter ion (Takeshima et al., 2015). Cl^-, K^+ and Mg^{2+} have all been proposed to fulfil this role, though there is currently no consensus as to which of these is the most important (Takeshima et al., 2015). The sarcoplasmic reticulum membrane expresses several Cl^- conductances, although their molecular identity is still in question (Takeshima et al., 2015). It is conceivable that the compounds we have discussed interfere with Ca^{2+} movements by blocking these channels, an idea that has previously been raised in airway smooth muscle (Hirota et al., 2006; Danielsson et al., 2015). Bestrophin-1 is another protein that forms Ca^{2+}-activated Cl^- channels, and several studies have shown that these are located in the endoplasmic reticulum membranes of epithelial cells, where they were proposed to provide the counter ion pathway for Ca^{2+} movements (Barro-Soria et al., 2010). It is notable that MONNA was shown to be

highly selective for TMEM16A over bestrophin-1 (Oh et al., 2013), so it is unlikely that its action on Ca^{2+} release in the present study was via blockade of bestrophin-1. Also, the fact that the elevations in Ca^{2+} caused by MONNA and benzbromarone occurred in Ca^{2+}-free bath solution, would suggest that they acted by causing Ca^{2+}-release rather by impeding sarcoplasmic reticulum Ca^{2+} movements. This conclusion is further supported by the fact that tetracaine and ryanodine both attenuated the action of benzbromarone.

Our results suggest that the TMEM16A blockers caused Ca^{2+} release by activating ryanodine receptors. This could have been due to a direct action on the ryanodine receptors, or an indirect effect as a result of causing release from a different intracellular Ca^{2+} store that then resulted in Ca^{2+}-induced Ca^{2+} release from the sarcoplasmic reticulum. Several TMEM16A blockers (niflumic acid, benzbromarone and niclosamide) are also mitochondrial toxins and would therefore be expected to interfere with mitochondrial Ca^{2+} handling, which could result in Ca^{2+}-induced Ca^{2+} release (McDougall et al., 1988; Felser et al., 2014; Tao et al., 2014; Shirakawa et al., 2015). However, there is strong evidence that some classical Cl^- channel blockers, including disulfonic stilbene derivatives, DIDS and SITS (4-acetoamido-4-′-isothiocyanostilbene-2,2′-disulfonic acid) and niflumic acid, directly alter the gating properties of ryanodine receptors inserted in lipid bilayers, usually with the effect of increasing their open probability (Zahradnikova and Zahradnik, 1993; Oba et al., 1996; Oba, 1997; Hill and Sitsapesan, 2002). As far as we are aware, no one has examined possible similar actions of the second generation of TMEM16A blockers on ryanodine receptor function, though clearly this would be of value.

In conclusion, we have demonstrated that three commonly used ‘new generation’ TMEM16A blockers caused Ca^{2+} release in airway smooth muscle cells, while a fourth blocker, Ani9, did not. Unlike the other blockers, Ani9 had no effect on carbachol induced contractions. Previous studies that have used these and similar compounds as tools to determine the role of TMEM16A in whole tissue experiments may have come to misleading conclusions and should be re-evaluated. Our work adds to the increasing body of literature that many TMEM16A blockers have off-target effects and therefore must be used cautiously.

Funding

This work was part of the BREATH (Border and REgions Airways Training Hub) project, funded by the European Union Interreg VA Research and Innovation (Health and Life Science) Programme. INTVA/045.

CRediT authorship contribution statement

Ritu Dwivedi: Conceptualization, Investigation, Formal analysis, Data curation, Visualization. **Bernard T. Drumm:** Conceptualization, Writing – review & editing, Formal analysis, Data curation, Visualization. **Tuleen Alkawadri:** Data curation. **S. Lorraine Martin:** Conceptualization, Writing – review & editing, Funding acquisition. **Gerard P. Sergeant:** Conceptualization, Resources, Writing – review & editing, Funding acquisition. **Mark A. Hollywood:** Conceptualization, Resources, Writing – review & editing, Funding acquisition. **Keith D. Thornbury:** Conceptualization, Formal analysis, Resources, Data curation, Writing – original draft, Writing – review & editing, Visualization, Supervision, Project administration, Funding acquisition.

Declaration of competing interest

There are no Conflicts of Interest.

Data availability

Data will be made available on request.

Acknowledgements

The authors are grateful for technical support provided by Billie McIlveen

Appendix A. Supplementary data

Supplementary data to this article can be found online at https://doi.org/10.1016/j.ejphar.2023.175677.

References

Barro-Soria, R., Aldehni, F., Almaca, J., Witzgall, R., Schreiber, R., Kunzelmann, K., 2010. ER-localized bestrophin 1 activates Ca2+-dependent ion channels TMEM16A and SK4 possibly by acting as a counterion channel. Pflügers Archiv 459, 485–497.
Boedtkjer, D.M., Kim, S., Jensen, A.B., Matchkov, V.M., Andersson, K.E., 2015. New selective inhibitors of calcium-activated chloride channels - T16A(inh) -A01, CaCC (inh) -A01 and MONNA - what do they inhibit? Br. J. Pharmacol. 172, 4158–4172.
Bradley, E., Fedigan, S., Webb, T., Hollywood, M.A., Thornbury, K.D., McHale, N.G., Sergeant, G.P., 2014. Pharmacological characterization of TMEM16A currents. Channels 8, 308–320.
Butler, G.B., Adler, K.B., Evans, J.N., Morgan, D.W., Szarek, J.L., 1987. Modulation of rabbit airway smooth muscle responsiveness by respiratory epithelium. Involvement of an inhibitory metabolite of arachidonic acid. Am. Rev. Respir. Dis. 135, 1099–1104.
Caputo, A., Caci, E., Ferrera, L., Pedemonte, N., Barsanti, C., Sondo, E., Pfeffer, U., Ravazzolo, R., Zegarra-Moran, O., Galietta, L.J., 2008. TMEM16A, a membrane protein associated with calcium-dependent chloride channel activity. Science 322, 590–594.
Centeio, R., Cabrita, I., Benedetto, R., Talbi, K., Ousingsawat, J., Schreiber, R., Sullivan, J.K., Kunzelmann, K., 2020. Pharmacological inhibition and activation of the Ca(2+) activated Cl(-) channel TMEM16A. Int. J. Mol. Sci. 21.
Cobine, C.A., Hannah, E.E., Zhu, M.H., Lyle, H.E., Rock, J.R., Sanders, K.M., Ward, S.M., Keef, K.D., 2017. ANO1 in intramuscular interstitial cells of Cajal plays a key role in the generation of slow waves and tone in the internal anal sphincter. J. Physiol. 595, 2021–2041.
Cruickshank, S.F., Baxter, L.M., Drummond, R.M., 2003. The Cl(-) channel blocker niflumic acid releases Ca(2+) from an intracellular store in rat pulmonary artery smooth muscle cells. Br. J. Pharmacol. 140, 1442–1450.
Danahay, H., Fox, R., Lilley, S., Charlton, H., Adley, K., Christie, L., Ansari, E., Ehre, C., Flen, A., Tuvim, M.J., Dickey, B.F., Williams, C., Beaudoin, S., Collingwood, S.P., Gosling, M., 2020a. Potentiating TMEM16A does not stimulate airway mucus secretion or bronchial and pulmonary arterial smooth muscle contraction. FASEB Bioadv 2, 464–477.
Danahay, H.L., Lilley, S., Fox, R., Charlton, H., Sabater, J., Button, B., McCarthy, C., Collingwood, S.P., Gosling, M., 2020b. TMEM16A potentiation: a novel therapeutic approach for the treatment of cystic fibrosis. Am. J. Respir. Crit. Care Med. 201, 946–954.
Danielsson, J., Perez-Zoghbi, J., Bernstein, K., Barajas, M.B., Zhang, Y., Kumar, S., Sharma, P.K., Gallos, G., Emala, C.W., 2015. Antagonists of the TMEM16A calcium-activated chloride channel modulate airway smooth muscle tone and intracellular calcium. Anesthesiology 123, 569–581.
De La Fuente, R., Namkung, W., Mills, A., Verkman, A.S., 2008. Small-molecule screen identifies inhibitors of a human intestinal calcium-activated chloride channel. Mol. Pharmacol. 73, 758–768.
Deba, F., Bessac, B.F., 2015. Anoctamin-1 Cl(-) channels in nociception: activation by an N-aroylaminothiazole and capsaicin and inhibition by T16A[inh]-A01. Mol. Pain 11, 55.
Drumm, B.T., Hannigan, K.I., Lee, J.Y., Rembetski, B.E., Baker, S.A., Koh, S.D., Cobine, C. A., Sanders, K.M., 2022. Ca(2+) signalling in interstitial cells of Cajal contributes to generation and maintenance of tone in mouse and monkey lower esophageal sphincters. J. Physiol. 600, 2613–2636.
Drumm, B.T., Hennig, G.W., Baker, S.A., Sanders, K.M., 2019a. Applications of spatio-temporal mapping and particle analysis techniques to quantify intracellular Ca 2+ signaling in situ. JoVE 2019, 1–13.
Drumm, B.T., Hwang, S.J., Baker, S.A., Ward, S.M., Sanders, K.M., 2019b. Ca2+ signalling behaviours of intramuscular interstitial cells of Cajal in the murine colon. J. Physiol. 597, 3587–3617.
Drumm, B.T., Rembetski, B.E., Baker, S.A., Sanders, K.M., 2019c. Tonic inhibition of murine proximal colon is due to nitrergic suppression of Ca 2+ signaling in interstitial cells of Cajal. Sci. Rep. 9, 1–14.
Drumm, B.T., Rembetski, B.E., Huynh, K., Nizar, A., Baker, S.A., Sanders, K.M., 2020a. Excitatory cholinergic responses in mouse colon intramuscular interstitial cells of Cajal are due to enhanced Ca(2+) release via M3 receptor activation. Faseb. J. 34, 10073–10095.
Drumm, B.T., Rembetski, B.E., Messersmith, K., Manierka, M.S., Baker, S.A., Sanders, K. M., 2020b. Pacemaker function and neural responsiveness of subserosal interstitial cells of Cajal in the mouse colon. J. Physiol. 598, 651–681.
Faudone, G., Arifi, S., Merk, D., 2021. The medicinal chemistry of caffeine. J. Med. Chem. 64, 7156–7178.
Fedigan, S., Bradley, E., Webb, T., Large, R.J., Hollywood, M.A., Thornbury, K.D., McHale, N.G., Sergeant, G.P., 2017. Effects of new-generation TMEM16A inhibitors

on calcium-activated chloride currents in rabbit urethral interstitial cells of Cajal. Pflueg. Arch. Eur. J. Physiol. 469, 1443–1455.
Felser, A., Lindinger, P.W., Schnell, D., Kratschmar, D.V., Odermatt, A., Mies, S., Jeno, P., Krahenbuhl, S., 2014. Hepatocellular toxicity of benzbromarone: effects on mitochondrial function and structure. Toxicology 324, 136–146.
Galietta, L.J.V., 2022. TMEM16A (ANO1) as a therapeutic target in cystic fibrosis. Curr. Opin. Pharmacol. 64, 102206.
Gallos, G., Remy, K.E., Danielsson, J., Funayama, H., Fu, X.W., Chang, H.Y., Yim, P., Xu, D., Emala, C.W., Sr ., 2013. Functional expression of the TMEM16 family of calcium-activated chloride channels in airway smooth muscle. Am. J. Physiol. Lung Cell Mol. Physiol. 305, L625–L634.
Gao, J., Yin, H., Dong, Y., Wang, X., Liu, Y., Wang, K., 2023. A novel role of uricosuric agent benzbromarone in BK channel activation and reduction of airway smooth muscle contraction. Mol. Pharmacol. 103, 241–254.
Genovese, M., Buccirossi, M., Guidone, D., De Cegli, R., Sarnataro, S., di Bernardo, D., Galietta, L.J.V., 2023. Analysis of inhibitors of the anoctamin-1 chloride channel (transmembrane member 16A, TMEM16A) reveals indirect mechanisms involving alterations in calcium signalling. Br. J. Pharmacol. 180, 775–785.
Greenwood, I.A., Large, W.A., 1995. Comparison of the effects of fenamates on Ca-activated chloride and potassium currents in rabbit portal vein smooth muscle cells. Br. J. Pharmacol. 116, 2939–2948.
Greenwood, I.A., Leblanc, N., 2007. Overlapping pharmacology of Ca2+-activated Cl- and K+ channels. Trends Pharmacol. Sci. 28, 1–5.
Gyorke, S., Lukyanenko, V., Gyorke, I., 1997. Dual effects of tetracaine on spontaneous calcium release in rat ventricular myocytes. J. Physiol. 500 (Pt 2), 297–309.
Hannigan, K.I., Griffin, C.S., Large, R.J., Sergeant, G.P., Hollywood, M.A., McHale, N.G., Thornbury, K.D., 2017. The role of Ca(2+)-activated Cl(-) current in tone generation in the rabbit corpus cavernosum. Am. J. Physiol. Cell Physiol. 313, C475–C486.
Hill, A.P., Sitsapesan, R., 2002. DIDS modifies the conductance, gating, and inactivation mechanisms of the cardiac ryanodine receptor. Biophys. J. 82, 3037–3047.
Hirota, S., Trimble, N., Pertens, E., Janssen, L.J., 2006. Intracellular Cl- fluxes play a novel role in Ca2+ handling in airway smooth muscle. Am. J. Physiol. Lung Cell Mol. Physiol. 290, L1146–L1153.
Huang, F., Rock, J.R., Harfe, B.D., Cheng, T., Huang, X., Jan, Y.N., Jan, L.Y., 2009. Studies on expression and function of the TMEM16A calcium-activated chloride channel. Proc. Natl. Acad. Sci. U. S. A. 106, 21413–21418.
Huang, F., Zhang, H., Wu, M., Yang, H., Kudo, M., Peters, C.J., Woodruff, P.G., Solberg, O.D., Donne, M.L., Huang, X., Sheppard, D., Fahy, J.V., Wolters, P.J., Hogan, B.L.M., Finkbeiner, W.E., Li, M., Jan, Y.N., Jan, L.Y., Rock, J.R., 2012. Calcium-activated chloride channel TMEM16A modulates mucin secretion and airway smooth muscle contraction. Proc. Natl. Acad. Sci. USA 109, 16354–16359.
Janssen, L.J., Sims, S.M., 1992. Acetylcholine activates non-selective cation and chloride conductances in canine and Guinea-pig tracheal myocytes. J. Physiol. 453, 197–218.
Koh, S.D., Drumm, B.T., Lu, H., Kim, H.J., Ryoo, S.B., Kim, H.U., Lee, J.Y., Rhee, P.L., Wang, Q., Gould, T.W., Heredia, D., Perrino, B.A., Hwang, S.J., Ward, S.M., Sanders, K.M., 2022. Propulsive colonic contractions are mediated by inhibition-driven poststimulus responses that originate in interstitial cells of Cajal. Proc. Natl. Acad. Sci. U. S. A. 119, e2123020119.
Liu, Y., Liu, Z., Wang, K., 2021. The Ca(2+)-activated chloride channel ANO1/TMEM16A: an emerging therapeutic target for epithelium-originated diseases? Acta Pharm. Sin. B 11, 1412–1433.
MacMillan, D., Chalmers, S., Muir, T.C., McCarron, J.G., 2005. IP3-mediated Ca2+ increases do not involve the ryanodine receptor, but ryanodine receptor antagonists reduce IP3-mediated Ca2+ increases in Guinea-pig colonic smooth muscle cells. J. Physiol. 569, 533–544.
McDougall, P., Markham, A., Cameron, I., Sweetman, A.J., 1988. Action of the nonsteroidal anti-inflammatory agent, flufenamic acid, on calcium movements in isolated mitochondria. Biochem. Pharmacol. 37, 1327–1330.
Miner, K., Labitzke, K., Liu, B., Wang, P., Henckels, K., Gaida, K., Elliott, R., Chen, J.J., Liu, L., Leith, A., Trueblood, E., Hensley, K., Xia, X.Z., Homann, O., Bennett, B., Fiorino, M., Whoriskey, J., Yu, G., Escobar, S., Wong, M., Born, T.L., Budelsky, A., Comeau, M., Smith, D., Phillips, J., Johnston, J.A., McGivern, J.G., Weikl, K., Powers, D., Kunzelmann, K., Mohn, D., Hochheimer, A., Sullivan, J.K., 2019. Drug repurposing: the anthelmintics niclosamide and nitazoxanide are potent TMEM16A antagonists that fully bronchodilate airways. Front. Pharmacol. 10, 51.
Nagasaki, K., Fleischer, S., 1988. Ryanodine sensitivity of the calcium release channel of sarcoplasmic reticulum. Cell Calcium 9, 1–7.
Namkung, W., Phuan, P.W., Verkman, A.S., 2011. TMEM16A inhibitors reveal TMEM16A as a minor component of calcium-activated chloride channel conductance in airway and intestinal epithelial cells. J. Biol. Chem. 286, 2365–2374.
Oba, T., 1997. Niflumic acid differentially modulates two types of skeletal ryanodine-sensitive Ca(2+)-release channels. Am. J. Physiol. 273, C1588–C1595.
Oba, T., Koshita, M., Van Helden, D.F., 1996. Modulation of frog skeletal muscle Ca2+ release channel gating by anion channel blockers. Am. J. Physiol. 271, C819–C824.
Oh, S.J., Hwang, S.J., Jung, J., Yu, K., Kim, J., Choi, J.Y., Hartzell, H.C., Roh, E.J., Lee, C. J., 2013. MONNA, a potent and selective blocker for transmembrane protein with unknown function 16/anoctamin-1. Mol. Pharmacol. 84, 726–735.
Ottolia, M., Toro, L., 1994. Potentiation of large conductance KCa channels by niflumic, flufenamic, and mefenamic acids. Biophys. J. 67, 2272–2279.
Paulino, C., Kalienkova, V., Lam, A.K.M., Neldner, Y., Dutzler, R., 2017a. Activation mechanism of the calcium-activated chloride channel TMEM16A revealed by cryo-EM. Nature 552, 421–425.
Paulino, C., Neldner, Y., Lam, A.K., Kalienkova, V., Brunner, J.D., Schenck, S., Dutzler, R., 2017b. Structural basis for anion conduction in the calcium-activated chloride channel TMEM16A. Elife 6.
Sathish, V., Leblebici, F., Kip, S.N., Thompson, M.A., Pabelick, C.M., Prakash, Y.S., Sieck, G.C., 2008. Regulation of sarcoplasmic reticulum Ca2+ reuptake in porcine airway smooth muscle. Am. J. Physiol. Lung Cell Mol. Physiol. 294.
Schroeder, B.C., Cheng, T., Jan, Y.N., Jan, L.Y., 2008. Expression cloning of TMEM16A as a calcium-activated chloride channel subunit. Cell 134, 1019–1029.
Seo, Y., Lee, H.K., Park, J., Jeon, D.K., Jo, S., Jo, M., Namkung, W., 2016. Ani9, a novel potent small-molecule ANO1 inhibitor with negligible effect on ANO2. PLoS One 11.
Sergeant, G.P., Craven, M., Hollywood, M.A., McHale, N.G., Thornbury, K.D., 2009. Spontaneous Ca2+waves in rabbit corpus cavernosum: modulation by nitric oxide and cGMP. J. Sex. Med. 6, 958–966.
Shirakawa, M., Sekine, S., Tanaka, A., Horie, T., Ito, K., 2015. Metabolic activation of hepatotoxic drug (benzbromarone) induced mitochondrial membrane permeability transition. Toxicol. Appl. Pharmacol. 288, 12–18.
Simmerman, H.K., Jones, L.R., 1998. Phospholamban: protein structure, mechanism of action, and role in cardiac function. Physiol. Rev. 78, 921–947.
Takayama, Y., Uta, D., Furue, H., Tominaga, M., 2015. Pain-enhancing mechanism through interaction between TRPV1 and anoctamin 1 in sensory neurons. Proc. Natl. Acad. Sci. U. S. A. 112, 5213–5218.
Takeshima, H., Venturi, E., Sitsapesan, R., 2015. New and notable ion-channels in the sarcoplasmic/endoplasmic reticulum: do they support the process of intracellular Ca (2)(+) release? J. Physiol. 593, 3241–3251.
Tao, H., Zhang, Y., Zeng, X., Shulman, G.I., Jin, S., 2014. Niclosamide ethanolamine-induced mild mitochondrial uncoupling improves diabetic symptoms in mice. Nat. Med. 20, 1263–1269.
Viero, C., Thomas, N.L., Euden, J., Mason, S.A., George, C.H., Williams, A.J., 2012. Techniques and methodologies to study the ryanodine receptor at the molecular, subcellular and cellular level. Adv. Exp. Med. Biol. 740, 183–215.
Wang, H.S., Dixon, J.E., McKinnon, D., 1997. Unexpected and differential effects of Cl-channel blockers on the Kv4.3 and Kv4.2 K+ channels. Implications for the study of the I(to2) current. Circ. Res. 81, 711–718.
Wang, P., Zhao, W., Sun, J., Tao, T., Chen, X., Zheng, Y.Y., Zhang, C.H., Chen, Z., Gao, Y. Q., She, F., Li, Y.Q., Wei, L.S., Lu, P., Chen, C.P., Zhou, J., Wang, D.Q., Chen, L., Shi, X.H., Deng, L., ZhuGe, R., Chen, H.Q., Zhu, M.S., 2018. Inflammatory mediators mediate airway smooth muscle contraction through a G protein-coupled receptor-transmembrane protein 16A-voltage-dependent Ca(2+) channel axis and contribute to bronchial hyperresponsiveness in asthma. J. Allergy Clin. Immunol. 141, 1259–1268 e1211.
Wang, W., 2018. Optogenetic manipulation of ENS - the brain in the gut. Life Sci. 192, 18–25.
Yang, Y.D., Cho, H., Koo, J.Y., Tak, M.H., Cho, Y., Shim, W.S., Park, S.P., Lee, J., Lee, B., Kim, B.M., Raouf, R., Shin, Y.K., Oh, U., 2008. TMEM16A confers receptor-activated calcium-dependent chloride conductance. Nature 455, 1210–1215.
Zahradnikova, A., Zahradnik, I., 1993. Modification of cardiac Ca2+ release channel gating by DIDS. Pflügers Archiv 425, 555–557.
Zhang, C.H., Li, Y., Zhao, W., Lifshitz, L.M., Li, H., Harfe, B.D., Zhu, M.S., ZhuGe, R., 2013. The transmembrane protein 16A Ca2+-activated Cl channel in airway smooth muscle contributes to airway hyperresponsiveness. Am. J. Respir. Crit. Care Med. 187, 374–381.